

A Three-Step Approach for Assessing Landscape Connectivity via Simulated Dispersal: African Wild Dog Case Study

David D. Hofmann^{1,2,§}  Gabriele Cozzi^{1,2}  John W. McNutt²
Arpat Ozgul¹  Dominik M. Behr^{1,2} 

April 7, 2022

¹ Department of Evolutionary Biology and Environmental Studies, University of Zurich,
Winterthurerstrasse 190, 8057 Zurich, Switzerland.

² Botswana Predator Conservation Program, Private Bag 13, Maun, Botswana.

§ Corresponding author (david.hofmann2@uzh.ch)

Running Title: Simulating Wild Dog Dispersal Trajectories to Assess Landscape
Connectivity

Keywords: dispersal, simulation, movement, integrated step-selection function,
Kavango-Zambezi Transfrontier Conservation Area, landscape connectivity, *Lycaon pictus*

Abstract

Context Dispersal of individuals contributes to long-term population persistence, yet requires a sufficient degree of landscape connectivity. To date, connectivity has mainly been investigated using least-cost analysis and circuit theory, two methods that make assumptions that are hardly applicable to dispersal. While these assumptions can be relaxed by explicitly simulating dispersal trajectories across the landscape, a unified approach for such simulations is lacking.

Objectives Here, we propose and apply a simple three-step approach to simulate dispersal and to assess connectivity using empirical GPS movement data and a set of habitat covariates.

Methods In step one of the proposed approach, we use integrated step-selection functions to fit a mechanistic movement model describing habitat and movement preferences of dispersing individuals. In step two, we apply the parameterized model to simulate dispersal across the study area. In step three, we derive three complementary connectivity maps; a heatmap highlighting frequently traversed areas, a betweenness map pinpointing dispersal corridors, and a map of inter-patch connectivity indicating the presence and intensity of functional links between habitat patches. We demonstrate the applicability of the proposed three-step approach in a case study in which we use GPS data collected on dispersing African wild dogs (*Lycaon pictus*) inhabiting northern Botswana.

Results Using step-selection functions we successfully parametrized a detailed dispersal model that described dispersing individuals' habitat and movement preferences, as well as potential interactions among the two. The model substantially outperformed a model that omitted such interactions and enabled us to simulate 80,000 dispersal trajectories across the study area.

Conclusion By explicitly simulating dispersal trajectories, our approach not only requires fewer unrealistic assumptions about dispersal, but also permits the calculation of multiple connectivity metrics that together provide a comprehensive view of landscape connectivity. In our case study, the three derived connectivity maps revealed several wild dog dispersal hotspots and corridors across the extent of our study area. Each map highlighted a different aspect of landscape connectivity, thus emphasizing their complementary nature. Overall, our case study demonstrates that a simulation-based approach offers a simple yet powerful alternative to traditional connectivity modeling techniques. It is therefore useful for a variety of applications in ecological, evolutionary, and conservation research.

1 Introduction

2 Dispersal of individuals is a vital process that allows species to maintain genetic diversity
3 (Perrin and Mazalov, 2000; Frankham et al., 2002; Leigh et al., 2012; Baguette et al., 2013),
4 rescue non-viable populations (Brown and Kodric-Brown, 1977), and to colonize unoccupied
5 habitats (Hanski, 1999; MacArthur and Wilson, 2001). However, the ability to disperse de-
6 pends on a sufficient degree of landscape connectivity (Fahrig, 2003; Clobert et al., 2012),
7 making the identification and protection of dispersal corridors that promote connectivity
8 a task of fundamental importance (Doerr et al., 2011; Rudnick et al., 2012). Identifying
9 dispersal corridors not only necessitates a comprehensive understanding of the factors that
10 limit dispersal, but also an appropriate model to estimate connectivity (Baguette et al., 2013;
11 Vasudev et al., 2015; Hofmann et al., 2021a). To date, the most commonly used connectivity
12 models are least-cost path analysis (LCPA; Adriaensen et al., 2003) and circuit theory (CT;
13 McRae, 2006; McRae et al., 2008). Unfortunately, both models rest on assumptions that
14 appear unsuitable for dispersers, thus calling for the development of alternative approaches.
15 One promising alternative is to assess landscape connectivity via simulated dispersal tra-
16 jectories generated from individual-based movement models (IBMMs, Diniz et al., 2019).
17 However, IBMMs require a large number of subjective modeling decisions, thus making
18 among-system comparisons difficult.

19 Traditional connectivity models make assumptions that are rarely met for dispersers.
20 LCPA, for instance, assumes that individuals move towards a preconceived endpoint and
21 choose a cost-minimizing route accordingly (Sawyer et al., 2011; Abrahms et al., 2017).
22 While this assumption may be justifiable for migrating animals, it is unlikely to hold for
23 dispersers, as dispersers typically move across unfamiliar territory towards an unknown end-
24 point (Koen et al., 2014; Cozzi et al., 2020). CT, on the contrary, posits that animals move
25 according to a random walk, entailing that autocorrelation between subsequent movements
26 cannot be rendered (Diniz et al., 2019). For dispersers, however, autocorrelated movements
27 are regularly observed (Cozzi et al., 2020; Hofmann et al., 2021a), meaning that dispersal
28 trajectories are usually strongly directional. Moreover, because both models require static
29 permeability or resistance surfaces as input, they are unable to reflect the temporal di-
30 mension of dispersal and therefore fail to allow statements about the expected duration for
31 moving between habitat patches (Martensen et al., 2017; Diniz et al., 2019).

32 The shortcomings inherent to LCPA and CT can be overcome by simulating dispersal
33 using IBMMs and by converting simulated trajectories into meaningful measures of connec-
34 tivity (Diniz et al., 2019). In contrast to LCPA and CT, IBMMs allow to explicitly simulate

35 how individuals move across and interact with the encountered landscape (Kanagaraj et al.,
36 2013; Clark et al., 2015; Allen et al., 2016; Hauenstein et al., 2019; Zeller et al., 2020), as
37 well as to render potential interactions between movement behavior and habitat conditions
38 (Avgar et al., 2016). This strictly shifts the focus from a structural to a more functional view
39 on connectivity (Tischendorf and Fahrig, 2000). Furthermore, IBMMs generate movement
40 sequentially, i.e. they generate a series of steps, so that the temporal dimension of dispersal
41 becomes explicit and allows modeling autocorrelation between successive steps (Diniz et al.,
42 2019). Finally, simulations from IBMMs do not enforce movement or connections towards
43 preconceived endpoints but allow individuals to adjust their route “on the go”, thereby
44 preventing biases arising from misplaced endpoints. Despite these advantages, a unifying
45 approach to simulate dispersal and assess connectivity using IBMMs is lacking. Considering
46 the large number of subjective decisions entailed by IBMMs, an approach that streamlines
47 and standardizes the application of dispersal simulations to assess connectivity will, however,
48 be critical to safeguard comparability among studies.

49 Here, we propose and exemplify a simple three-step approach for simulating dispersal and
50 assessing landscape connectivity (Figure 1). In step one, we combine GPS movement data
51 of dispersing individuals with habitat covariates to fit a mechanistic movement model via in-
52 tegrated step-selection functions (ISSFs, Avgar et al., 2016). We chose to use ISSFs because
53 the framework not only allows inference on the study species’ habitat kernel (i.e. its habi-
54 tat preferences), but also its movement kernel (i.e. its movement preferences/capabilities)
55 and potential interactions among the two (Avgar et al., 2016; Fieberg et al., 2021). In
56 step two, we use the parametrized movement model to simulate dispersal across the study
57 area. Comparable simulations have already been applied to estimate steady-state utilization
58 distributions of resident individuals (Potts et al., 2013; Signer et al., 2017) and to model
59 landscape connectivity, yet disregarding interdependencies between habitat and movement
60 kernels (Clark et al., 2015; Zeller et al., 2020). Finally, in step three, we convert the simulated
61 trajectories into three complementary connectivity maps; (i) a heatmap revealing frequently
62 traversed areas (e.g. Hauenstein et al., 2019; Zeller et al., 2020), (ii) a betweenness-map
63 delineating dispersal corridors and bottlenecks (e.g. Bastille-Rousseau et al., 2018), (iii) and
64 a map of inter-patch connectivity, depicting the presence and intensity of functional links
65 between habitat patches, as well as the average dispersal duration required to realize those
66 connections (e.g. Gustafson and Gardner, 1996; Kanagaraj et al., 2013).

67 We showcase the application of the proposed approach using GPS movement data col-
68 lected on dispersing African wild dogs (*Lycaon pictus*). The African wild dog is a highly

mobile species whose population persistence heavily relies on the availability of large, natural or semi-natural landscapes and a sufficient degree of connectivity among remaining subpopulations. Once common throughout sub-Saharan Africa, this species has disappeared from much of its historic range, largely due to human persecution, habitat fragmentation, and disease outbreaks (Woodroffe and Sillero-Zubiri, 2012). Wild dogs typically disperse in single-sex coalitions (McNutt, 1996; Behr et al., 2020) and are capable of dispersing several hundred kilometers (Davies-Mostert et al., 2012; Masenga et al., 2016; Cozzi et al., 2020). Although previous studies have investigated connectivity for this species using LCPA (Hofmann et al., 2021a) and CT (Brennan et al., 2020), a more comprehensive and mechanistic understanding of dispersal and connectivity is missing (but see Creel et al., 2020). Nevertheless, with about 6,000 free-ranging wild dogs remaining in fragmented subpopulations (Woodroffe and Sillero-Zubiri, 2012), reliable information on dispersal behavior and landscape connectivity is essential for the conservation of this endangered carnivore. We anticipated that a connectivity assessment based upon our three-step approach would overcome several of the conceptual shortcomings of traditional connectivity models, while providing a more detailed view on movement behavior during dispersal its implications for landscape connectivity.

2 Methods

2.1 Case Study

2.1.1 GPS Data

We applied the three step approach presented in Figure 1 to GPS movement data from 16 dispersing African wild dog coalitions (7 female and 9 male coalitions). This data has been collected between 2011 and 2019 from a free-ranging wild dog population in northern Botswana. During dispersal, GPS collars recorded a fix every 4 hours and regularly transmitted data over the Iridium satellite system. To ensure comparable time intervals between GPS fixes, we removed any fixes that were not successfully obtained at the desired 4-hour schedule (allowing for a tolerance of \pm 15 minutes). To prepare the data for step-selection analysis, we converted the fixes ($n = 4'169$) into steps, where each step represented the straight-line movement between two consecutive GPS fixes (Turchin, 1998). We only considered steps with equal step-durations (i.e. 4 hours) for further analysis. We will refer to these steps as “realized steps”. Additional details on the data collection and preparation can be found in Cozzi et al. (2020) and Hofmann et al. (2021a).

101 **2.1.2 Study Area**

102 Our simulation of dispersal trajectories and assessment of connectivity spanned across the
103 entire Kavango-Zambezi Transfrontier Conservation Area (KAZA-TFCA, Figure 2a and b).
104 The KAZA-TFCA is the world's largest transboundary conservation area and comprises
105 parts of Angola, Botswana, Namibia, Zimbabwe, and Zambia, thus hosting a rich diversity
106 of landscapes, ranging from savannah to grassland and from dry to moist woodland habitats.
107 In its center lies the Okavango Delta, a dominant hydro-geographical feature and the world's
108 largest flood-pulsing inland delta. Large portions of the KAZA-TFCA are formally protected
109 in the form of national parks (NPs) or other protected areas, yet a considerable portion of
110 the landscape remains human-dominated (e.g. roads, agricultural sites, and settlements).

111 **2.1.3 Habitat Covariates**

112 We represented the physical landscape in our study area by the habitat covariates `water-`
113 `cover`, `distance-to-water`, `woodland-cover`, `shrub/grassland-cover`, and `human-influence`. To
114 render the seasonal dynamics of water-cover for the extent of the Okavango Delta, we
115 applied an algorithm that enabled us to obtain weekly updated raster-layers for `water-`
116 `cover` and `distance-to-water` from MODIS satellite imagery (Wolski et al., 2017; Hofmann
117 et al., 2021a). This algorithm is now implemented in the `floodmapr` package (available on
118 GitHub; <https://github.com/DavidDHofmann/floodmapr>). To ensure a consistent resolu-
119 tion across habitat covariates, we coarsened or interpolated all layers to a resolution of 250
120 m x 250 m. A detailed description of how we prepared each habitat covariate is provided in
121 Hofmann et al. (2021a).

122 We performed all data preparations, spatial computations, and statistical analysis in
123 R, version 3.6.6 (R Core Team, 2020). Some helper functions were written in C++ and
124 imported into R using the `Rcpp` package (Eddelbuettel and François, 2011; Eddelbuettel,
125 2013; Eddelbuettel and Balamuta, 2018).

126 **2.2 Step 1 - Movement Model**

127 We combined the collected GPS data with habitat covariates and used ISSFs (Avgar et al.,
128 2016) to parametrize a mechanistic movement model. More specifically, we paired each
129 realized step with a set of 24 randomly generated alternative steps. A realized and its 24
130 random steps together formed a stratum that received a unique identifier. As suggested by
131 Avgar et al. (2016), we generated random steps by sampling random turning angles from a
132 uniform distribution $(-\pi, +\pi)$ and step lengths from a gamma distribution that was fitted

133 to realized steps (scale $\theta = 6'308$ and shape $k = 0.37$). Note that our approach of sampling
 134 turning angles from a uniform distribution does not imply that we assume uniform turning
 135 angles, as we will account for directionality later in the model (Avgar et al., 2016; Fieberg
 136 et al., 2021).

137 Along each realized and random step, we extracted values from underlying habitat covari-
 138 ate layers and we computed averages of each covariate along the steps. Besides extracting
 139 *habitat covariates*, we also computed movement metrics that we used as *movement covari-
 140 ates* in the ISSF models (Avgar et al., 2016; Fieberg et al., 2021). Specifically, we computed
 141 the step length (`sl`), its natural logarithm (`log(sl)`), and the cosine of the relative turning
 142 angle (`cos(ta)`), which is a measure of directionality (Turchin, 1998), for each step. Because
 143 wild dog activity is low during the hot midday hours (Cozzi et al., 2012), we additionally
 144 created the variable `LowActivity`, indicating whether a step was realized during periods of
 145 low wild dog activity (09:00 to 17:00 local time) or high wild dog activity (17:00 to 09:00
 146 local time). To facilitate model convergence, we standardized all continuous covariates to
 147 a mean of zero and a standard deviation of one. Correlations among covariates were low
 148 ($|r| < 0.6$; Latham et al., 2011), so we retained all of them for modeling.

149 To contrast realized steps (scored 1) and random steps (scored 0), we assumed that
 150 animals assigned a selection score $w(x)$ to each step (Equation 1; Fortin et al., 2005), where
 151 $w(x)$ depended on the step's associated covariates (x_1, x_2, \dots, x_n) and on the animal's relative
 152 selection strengths Avgar et al., 2017 towards these covariates $(\beta_1, \beta_2, \dots, \beta_n)$:

$$w(x) = \exp(\beta_1 x_1 + \beta_2 x_2 + \dots + \beta_n x_n) \quad (\text{Equation 1})$$

153 The probability of a step i being realized was then contingent on the step's selection score,
 154 as well as on the selection scores of all other step in the same stratum:

$$P(Y_i = 1 | Y_1 + Y_2 + \dots + Y_i = 1) = \frac{w(x_i)}{w(x_1) + w(x_2) + \dots + w(x_i)} \quad (\text{Equation 2})$$

155 To estimate relative selection strengths (i.e. the β -coefficients), we used mixed effects con-
 156 ditional logistic regression analysis, implemented through the r-package `glmmTMB` (Brooks
 157 et al., 2017). The implementation of conditional logistic regression has been proposed by
 158 Muff et al. (2020) and allows to model random slopes. The method requires to fix the vari-
 159 ance of the stratum specific intercept to a large value, so we fixed it to an arbitrary high
 160 value of 10^6 and used disperser identity to model random slopes for all covariates.

Our movement model was based on a habitat selection model that was previously developed for dispersing wild dogs (hereafter referred to as *base model*, Hofmann et al., 2021a). In the base model, no interactions among habitat covariates and movement covariates were considered, so we here expanded the model and allowed for such interactions, acknowledging that movement preferences during dispersal could depend on habitat conditions (details in Appendix A1). To determine the most parsimonious movement model among model candidates, we ran stepwise forward model selection based on Akaike's Information Criterion (AIC, Burnham and Anderson, 2002). More specifically, we started with the base model and iteratively increased model complexity by adding all possible interactions between movement and habitat covariates. We validated the predictive power of the most parsimonious model using k-fold cross-validation for case-control studies as described in Fortin et al. (2009). This validation proves a significant prediction in case the Spearman rank correlation coefficient of predicted step-ranks and associated frequencies under the movement model is significantly greater than under the assumption of random preferences (details in Appendix A2).

2.3 Step 2 - Dispersal Simulation

We used the most parsimonious movement model to simulate individual dispersal trajectories across the study area. The simulation of a dispersal trajectory resembled an “inverted” ISSF and was set up as follows. (1) We defined a source point and assumed a random initial orientation of the simulated animal. (2) Starting from the source point, we generated 25 random steps by sampling turning angles from a uniform distribution $(-\pi, +\pi)$ and step lengths from our fitted gamma distribution. (3) Along each random step, we extracted and averaged values from the habitat covariate layers and we computed the movement metrics sl , $\log(sl)$, and $\cos(ta)$. To ensure compatible scales with the fitted movement model, we standardized covariate values using means and standard deviations from the empirical data. (4) We applied the parametrized movement model to predict the selection score $w(x)$ for each step using Equation 1 and we converted predicted scores into probabilities using Equation 2. (5) We randomly sampled one of the generated random steps based on assigned probabilities and determined the animal’s new position. We repeated steps (2) to (5) until 2,000 steps were realized and we repeated the simulation until a total of 80’000 dispersal trajectories was reached.

As source points for the simulations, we distributed 50,000 points at random locations inside protected areas that were large enough to host an average size wild dog home range (i.e. $> 700 \text{ km}^2$; Pomilia et al., 2015). We placed another 30,000 points randomly inside the

194 buffer zone, mimicking potential immigration into the study area (Figure S1).

195 To mitigate edge effects and to deal with random steps leaving the study area, we followed
196 Koen et al. (2010) and artificially expanded all covariate layers by a 100 km wide buffer
197 zone. Within the buffer zone, we randomized covariate values by resampling values from the
198 original covariate layers. Through this buffer zone, simulated dispersers were able to leave
199 and re-enter the main study area. In cases where random steps crossed the outer border of
200 this buffer zone, we resampled steps until they fully lied within the buffer zone, essentially
201 forcing simulated individuals to remain within the expanded study area.

202 To ensure reliable connectivity estimates, we determined the number of simulated dis-
203 persal trajectories required to reach a “steady state”. For this purpose, we distributed 1,000
204 rectangular “checkpoints”, each with an arbitrary extent of 5 km x 5 km, at random co-
205 ordinates within the study area (excluding the buffer). We then determined the relative
206 frequency at which each checkpoint was traversed by simulated dispersal trajectories (here-
207 after referred to as relative traversal frequency) as we gradually increased the number of
208 simulated trajectories from 1 to 50,000. To assess variability in the relative traversal fre-
209 quency, we repeatedly subsampled 100 times from all 50'000 trajectories and computed the
210 mean traversal frequency across replicates, as well as its 95% prediction-interval for each
211 checkpoint. We considered connectivity to have reached a steady state once the width of
212 the prediction-interval dropped below a value of 0.01 for all checkpoints.

213 **2.4 Step 3 - Connectivity Maps**

214 **2.4.1 Heatmap**

215 To identify dispersal hotspots within the study area, we created a heatmap indicating the
216 absolute frequency at which different areas were traversed by simulated dispersal trajectories
217 (e.g. Hauenstein et al., 2019; Zeller et al., 2020). Specifically, we rasterized all simulated
218 trajectories onto a raster with 1 km x 1 km resolution and tallied resulting layers into a
219 single map. This procedure ensured that every trajectory was only counted once, even if
220 it traversed the same raster-cell multiple times, thus reducing potential biases caused by
221 individuals that were surrounded by unfavorable habitat and “moved in circles”. To achieve
222 high performance rasterization, we used the R-package **terra** (Hijmans, 2021).

223 **2.4.2 Betweenness Map**

224 To pinpoint movement corridors and bottlenecks, we converted simulated trajectories into
225 a network and calculated betweenness scores for all raster-cells in the study area (Bastille-

Rousseau et al., 2018). Betweenness is a pertinent metric for connectivity as it measures how often a specific network-node (in our case a raster-cell) lies on a shortest path between any other pair of nodes (Bastille-Rousseau et al., 2018). To convert simulated trajectories into a network, we followed Bastille-Rousseau et al. (2018) and overlaid the study area (including the buffer) with a raster containing 5 km x 5 km raster-cells, where the center of each raster-cell served as node in the final network. To identify edges (i.e. connections) between the nodes, we used the simulated trajectories and determined all transitions occurring from one cell to another, as well as the frequency at which those transitions occurred. This resulted in an edge-list that we translated into a weighted network using the r-package `igraph` (Csardi and Nepusz, 2006). The final weight of each edge was determined by the frequency of transitions, yet because `igraph` handles edge weights (ω) as costs, we inverted the traversal-frequency through each raster-cell by applying $\omega = \frac{\text{mean}(\text{TraversalFrequency})}{\text{TraversalFrequency}_i}$. Consequently, regularly used edges received small weights (i.e. low costs) and vice versa. We used the weighted network to calculate betweenness scores for all network nodes.

2.4.3 Inter-Patch Connectivity Map

To examine the presence and intensity of functional links (i.e. connections) between patches within the study area, we calculated inter-patch connectivity (e.g. Gustafson and Gardner, 1996, Kanagaraj et al., 2013). For this, we computed the relative frequency at which dispersers originating from one patch successfully moved into another patch. We considered movements between patches as successful if an individual's dispersal trajectory originating from the source patch intersected with the target patch at least once. For each trajectory we also recorded the number of steps required to reach the first intersection with the respective patch, allowing us to compute the average dispersal durations from one patch to another. In summary, we determined *if* and *how often* dispersers moved between certain patches, as well as *how long* individuals had to move to make these connections. In our case study, we used NPs as patches to determine inter-patch connectivity, hence we'll use the terms interchangeably from here on. The decision to focus on NPs was purely out of simplicity and should not imply that dispersal between other areas is impossible.

3 Results

The most parsimonious movement model consisted of movement covariates, habitat covariates, as well as several of their interactions, thus suggesting that movement behavior during dispersal depended on habitat conditions (Figure 3a, Table S1 and Table S2). Although

multiple models received an AIC weight > 0 (Table S1), we only considered results from the most parsimonious model for simplicity. This decision only marginally influenced subsequent steps as all models with positive AIC weights retained similar covariates (Table S1). The k-fold cross-validation showed that the final model substantially outperformed a random guess and provided reliable predictions (i.e. confidence intervals of $\bar{r}_{s,realized}$ and $\bar{r}_{s,random}$ did not overlap). Moreover, the model correctly assigned high selection scores to realized steps (Figure 3b), indicating a good fit between predictions and observations. As can be taken from the Spearman rank correlation coefficient, the inclusion of several interactions between movement and habitat covariates significantly improved model performance ($\bar{r}_{s,realized} = -0.65; 95\% - CI = [-0.67, -0.64]$), compared to the base model ($\bar{r}_{s,realized} = -0.55; 95\% - CI = [-0.57, -0.52]$; Hofmann et al., 2021a)

Plots that aid with the interpretation of the most parsimonious movement model are provided in Figure S2 and suggest that, under average conditions, dispersing wild dogs avoided moving through water, woodlands, and areas dominated by humans, but preferred moving across shrublands or grasslands (Figure 3a). Dispersers realized shorter steps (indicating slower movements) in areas covered by water or woodland, while realizing larger steps in areas dominated by shrubs or grass (Figure 3a). We found a particularly large effect for the variable **LowActivity**, suggesting that dispersing wild dogs moved substantially faster during twilight and at night (i.e. between 17:00 and 09:00 o'clock; Figure 3a). Although dispersers revealed a preference for directional movements (i.e. low turning angles), especially when moving quickly, they did less so in proximity to humans or water, resulting in more tortuous movements in such areas (Figure 3a).

3.1 Dispersal Simulation

Dispersal simulations based on the most parsimonious movement model proved useful for assessing landscape connectivity. Of the 50,000 simulated dispersal trajectories that originated from the main study area, only 4.5% reached a map boundary, suggesting that we successfully mitigated biases from boundary effects. Moreover, our examination of the relative traversal frequency across all checkpoints showed that the relative traversal frequency reached a steady state after 10,500 simulated dispersal trajectories (Figure S3). Although variability in the relative traversal frequency kept decreasing as we increased the number of simulated dispersers, the marginal benefit of simulating additional trajectories diminished quickly (Figure S3).

290 **3.2 Heatmap**

291 The heatmap (Figure 4), which resulted from the summation of all simulated dispersal tra-
292 jectories, allowed us to pinpoint areas that were frequently visited and enabled us to compare
293 areas inside and outside the KAZA-TFCA borders with respect to the intensity at which they
294 were used for dispersal. For instance, we could deduct that areas inside the KAZA-TFCA
295 were frequently traversed by dispersers (median traversal frequency inside KAZA-TFCA
296 = 166, IQR = 274, Figure S6a), whereas areas beyond the KAZA-TFCA boundary were
297 comparatively rarely visited (median traversal frequency outside KAZA-TFCA = 61, IQR
298 = 133, Figure S6a). Most notably, the region in northern Botswana south of the Linyanti
299 swamp appeared to serve as highly frequented dispersal hotspot (median traversal frequency
300 = 987, IQR = 558). Aside from revealing movement hotspots, the heatmap also provided in-
301 formation on areas that appeared to hinder movement. For example, extensive water bodies,
302 such as the Okavango Delta, the Makgadikgadi Pan, and the Linyanti swamp, substantially
303 restricted dispersal movements and limited realized connectivity inside the KAZA-TFCA.
304 Similarly, the landscapes of Zambia and Zimbabwe were only rarely used for dispersal,
305 even within the KAZA-TFCA boundaries (Figure S7a). Despite the fact that the heatmap
306 improved our understanding of the frequency at which areas were traversed by simulated
307 dispersers, it seemed impractical to pinpoint dispersal corridors.

308 **3.3 Betweenness**

309 The betweenness map (Figure 5) revealed several distinct dispersal corridors that run across
310 the study area. In comparison to the heatmap, the betweenness map was less biased towards
311 areas with many dispersers and pronounced narrower, more linear routes that were used by
312 simulated individuals to move between regions. Again, northern Botswana emerged as a
313 wild dog dispersal corridor that connected more remote regions in the study area. Towards
314 east, the extension of this corridor ran through Chobe NP into Hwange NP. From there,
315 a further extension connected to Matusadona NP in Zimbabwe. Northwest of the Linyanti
316 ecosystem, a major corridor expanded into Angola, where it split and finally traversed over
317 a long stretch of unprotected area into Zambia's Kafue NP. Several additional corridors
318 with lower betweenness scores emerged, yet most of them ran within the KAZA-TFCA
319 boundaries (median betweenness inside KAZA-TFCA = 6.947×10^6 , IQR = 54.311×10^6 ,
320 Figure S6b). Consequently, only few corridors directly linked the peripheral regions of the
321 KAZA-TFCA and passed through unprotected areas outside its borders (mean betweenness
322 outside KAZA-TFCA = 2.685×10^6 , IQR = 9.891×10^6 , Figure S6b).

323 **3.4 Inter-Patch Connectivity**

324 The inter-patch connectivity map showed that the relative frequency at which simulated
325 dispersal trajectories moved from one patch to another varied, as did the average dispersal
326 duration between patches (Figure 6). The map thereby completed the picture on connectiv-
327 ity and provided valuable insights into the frequency and duration of connections between
328 patches. For some patches, we also detected imbalances between the number of incoming
329 and outgoing links, hinting at possible source-sink dynamics. From Chobe NP, for instance,
330 510 individuals reached the Moremi NP, yet the opposite route was only realized by 340
331 individuals. Relative to the number of simulated individuals, however, these numbers corre-
332 spond to fractions of 50% and 68%, respectively. Overall, inter-patch connectivity between
333 patches in Angola, Namibia, Botswana, and Zimbabwe appeared to be high; between 54%
334 and 87% of individuals originating from a patch in these countries successfully moved into
335 at least one other patch (Figure S8a). Conversely, only 19% of the dispersers leaving from
336 a patch in Zambia managed to find their way into some other patch (Figure S8b). Prior
337 to reaching another patch, individuals from Angola, Namibia, Botswana, Zimbabwe, and
338 Zambia had to move for an average of 630, 640, 940, 1045, and 890 steps, respectively. Fur-
339 thermore, it appeared that the corridor previously identified on Figure 6 between Angola’s
340 NPs and the Kafue NP in Zambia is only rarely realized.

341 **4 Discussion**

342 Here, we presented a simple three-step approach to assess landscape connectivity via simu-
343 lated dispersal trajectories and we demonstrated its application using empirical data from
344 a free-ranging population of African wild dogs. In step one, we used ISSFs to parametrize a
345 fully mechanistic movement model describing how individuals move through the landscape.
346 Aside from rendering habitat preferences, the model also encapsulated movement prefer-
347 ences and potential interactions between movement and habitat preferences. In step two,
348 we employed the movement model and simulated dispersal trajectories across the landscape.
349 In comparison to more traditional connectivity modeling techniques, such simulations re-
350 quire fewer unrealistic assumptions about dispersal and enable the derivation of multiple
351 connectivity metrics. Hence, in step three, we translated the simulated trajectories into
352 three complementary connectivity maps, each emphasizing a different aspect of landscape
353 connectivity (e.g. frequently traversed areas, critical dispersal corridors and bottlenecks,
354 and the presence and intensity of functional links between suitable patches).

Results on the habitat kernel from our model showed that dispersers avoided areas dominated by humans and covered by water, but selected for regions with open grassland in the vicinity to water bodies. This largely complied with previous studies that investigated habitat selection by dispersing wild dogs (Davies-Mostert et al., 2012; Masenga et al., 2016; Woodroffe et al., 2019; O'Neill et al., 2020; Hofmann et al., 2021a). However, instead of merely generating insights on dispersers' habitat preferences, the ISSF framework also permitted us to model several additional complexities common to dispersal. For instance, by including the interactions $\cos(\text{ta}):sl$ and $\cos(\text{ta}):\log(sl)$, we could accommodate that dispersers exhibit turning angles that are correlated with step lengths, meaning that turning angles tend to be smaller when individuals move fast. Although similar autocorrelations could be incorporated by sampling step lengths and turning angles from copula probability distributions (Hodel and Fieberg, 2022), the ISSF framework allowed us to conveniently model such peculiarities directly in the movement model. While we only considered first order autocorrelation, i.e. correlation between two consecutive steps, higher order autocorrelation is conceivable and may be desirable to model (Dray et al., 2010; McClintock et al., 2012). However, this will require vast amounts of GPS data that are not interrupted by missing fixes; something that is rarely achieved in reality (Graves and Waller, 2006). The power and flexibility of ISSFs to model additive effects between habitat and movement covariates (Avgar et al., 2016; Signer et al., 2017) furthermore allowed us to formally capture that dispersing wild dogs move slower and more tortuous in areas covered by water. Such effects may be of limited interest and novelty from a biological perspective, yet they are important to be considered when simulating dispersal, in particular if one is interested in estimating dispersal durations between habitat patches. Overall, the inclusion of interactions between habitat and movement covariates in our movement model lead to a significant improvement in predictive performance compared to an earlier model that omitted such interactions (Hofmann et al., 2021a).

Each of the three connectivity maps derived from simulated dispersal trajectories highlighted a different aspect of landscape connectivity. The heatmap was most suitable for pinpointing frequently traversed areas and showed that an exceptionally large number of dispersers moved through the regions of the Moremi NP and the Chobe NP in northern Botswana. Hofmann et al. (2021a) previously identified the same area as potential dispersal hotspot using LCPA, however, following their analysis it was not clear whether this was the consequence of the central location of the region and connections being enforced between predefined start and endpoints. Contrary to LCPA, a simulation-based approach as pre-

sented here does not require predefined endpoints, as endpoints emerge naturally from the simulated dispersal trajectories. This is especially useful for dispersal studies, where known endpoints are usually an unrealistic assumption (Elliot et al., 2014; Abrahms et al., 2017; Cozzi et al., 2020). The fact that the same region was emphasized using vastly different methods to model connectivity thus reinforces our notion that the area is of exceptional importance to dispersing wild dogs. Because simulated individuals are not forced to move towards certain endpoints, a simulation-based approach not only lends itself to study landscape connectivity, but also to uncover potential dispersal traps (Van der Meer et al., 2014) or areas with a high susceptibility for human wildlife conflicts (Cushman et al., 2018).

In contrast to the heatmap, the betweenness map emphasized relatively narrow and linear movement routes. It thus facilitated the identification of discrete movement corridors. While in some cases both the heatmap and the betweenness map attributed a high importance to the same areas (e.g. northern Botswana), little consensus was found for other regions. For instance, the stretch of unprotected land between Luengue-Luiana NP in Angola and the Kafue NP in Zambia was characterized by a high betweenness-scores, yet it only received low scores on the heatmap. This is due to the differential way in which the maps view connectivity. While the heatmap attributes a high connectivity to areas that are frequently traversed, it does not distinguish between areas that truly bring individuals into other regions of the study area and regions that lead into ecological traps. The converse is true on the betweenness map, as it strictly highlights regions that promote movement into other areas of the landscape and thus promote gene-flow. However, neither of the two maps provides insights into functional links between distinct habitat patches or how connections depend on the dispersal duration. For this reason, we also produced a map of inter-patch connectivity. This map depicted the frequency at which simulated individuals moved between patches as well as the average dispersal duration (in steps) required to realize them. Calculating dispersal durations was only possible because trajectories were simulated spatially and temporally explicitly, something that is currently unfeasible with LCPA or CT. An explicit representation of time enables answerings questions such as: “*How long will it take a disperser to move from A to B?*” or “*Is it possible for a disperser to move from A to B within X days?*”. Moreover, it yields opportunities to incorporate seasonality and to investigate whether dispersal corridors exist seasonally or all-year round (*dynamic connectivity*; Zeller et al., 2020). With LCPA or CT, seasonality can currently only be incorporated through the preparation of multiple permeability surfaces on which the same connectivity model is repeatedly applied (e.g. Osipova et al., 2019). With simulations from ISSFs, in contrast, the

423 environment could change “as the dispersers move”, so that simulated trajectories would
424 dynamically respond to seasonal fluctuations in the environment.

425 Despite the many benefits and great flexibility offered by simulations from ISSFs, one
426 must also be aware of the associated limitations. For example, while our approach of simulat-
427 ing dispersal proved useful to assess landscape connectivity, it was computationally costly.
428 Simulating 80,000 dispersal trajectories for 2'000 steps across the KAZA-TFCA required
429 five days of computation on a regular desktop machine (AMD Ryzen 7 2700X octa-core
430 processor with 3.6 GHz, 64 GB of RAM). The long simulation time was primarily caused
431 by the massive extent of the study area considered (ca. 1.8 Mio km²) and the large num-
432 ber of simulated trajectories. Most connectivity studies focus on smaller study areas (e.g.
433 Kanagaraj et al., 2013; Clark et al., 2015; McClure et al., 2016; Abrahms et al., 2017; Zeller
434 et al., 2020) and will therefore require fewer simulations and achieve faster simulation times
435 (given the same spatial resolution). We also believe that fewer simulated trajectories will
436 often suffice, as the relative traversal frequency by simulated trajectories through randomly
437 placed checkpoints across our study area converged already after 10,500 runs. The exact
438 number of required simulations to achieve reliable estimates of connectivity will, of course,
439 vary depending on the structure of the landscape and the dispersal capabilities of the focal
440 species (Gustafson and Gardner, 1996). For species that disperse short distances through
441 homogeneous environments, few simulations may suffice to gauge connectivity, whereas for
442 species that disperse over long distances through heterogeneous habitats, a large number of
443 simulations will be required to sufficiently explore the spectrum of possible routes.

444 Aside from the computational requirements, simulations further entail several non-trivial
445 but important modeling decisions. On four such decisions we would like to further elaborate:
446 (1) the number of simulated individuals, (2) the location of source points, (3) the simulated
447 dispersal duration, and (4) the behavior at map boundaries.

448 (1) When simulating dispersal trajectories, the modeler needs to decide on the number
449 of simulated individuals. A higher number is always desirable, as each additional trajectory
450 provides information about landscape connectivity. However, each additional simulation
451 imposes computational costs, so a trade-off needs to be managed. Signer et al. (2017)
452 proposed to handle the trade-off by simulating additional individuals only until the metrics
453 of interest converge towards a steady state. Here, we used the relative traversal frequency
454 as target metric and found that it converged already after 10'500 simulated individuals.
455 The exact number of required individuals might, however, vary depending on the employed
456 target metric and the anticipated connectivity map. More sophisticated target metrics than

457 the relative traversal frequency, preferably tailored to different connectivity maps, need to
458 be developed in the future.

459 (2) To initiate dispersers, a modeler needs to provide a set of source points at which
460 the virtual dispersers are released. We placed source points within protected areas large
461 enough to sustain viable wild dog populations, implicitly assuming that wild dogs primarily
462 survive in large, formally protected areas (Davies-Mostert et al., 2012; Woodroffe and Sillero-
463 Zubiri, 2012; Van der Meer et al., 2014). Moreover, we lacked precise knowledge about the
464 distribution and abundance of wild dogs across protected areas, so we placed source points
465 randomly within them. In cases where more detailed data distribution and abundance are
466 available, source points could be distributed accordingly. Alternatively, source points could
467 be distributed homogeneously but later be weighted when computing connectivity metrics.
468 In any case, the challenge of selecting meaningful source points is not unique to individual-
469 based simulations but also applies to LCPA and CT.

470 (3) The use of ISSFs to simulate dispersers requires deciding on the number of simulated
471 steps (i.e. the simulated dispersal durations). If sufficient dispersal data of the focal species
472 has been collected, dispersal durations could be sampled from observed dispersal events or
473 from parametric distributions fit to observed data. Due to the low number of observed
474 dispersal events, we opted against this solution and instead simulated all individuals for
475 2,000 steps, which was at the upper end of observed dispersal durations in African wild
476 dogs (Davies-Mostert et al., 2012; Masenga et al., 2016; Cozzi et al., 2020; Hofmann et al.,
477 2021a). This approach had the advantage that it allowed us to systematically shorten the
478 simulated trajectories after their simulation and thereby to investigate the sensitivity of our
479 results with respect to exact dispersal durations (Figures S4 and S5).

480 (4) Unless simulated dispersal trajectories are strongly drawn towards a point of attrac-
481 tion inside the study area(e.g. Signer et al., 2017), some trajectories will inevitably approach
482 one of the map boundaries. In this case, one or more of the generated random steps might
483 leave the study area, making it impossible to compute a selection score. A possible solution
484 is to simply terminate the simulation affected trajectory, assuming that the simulated indi-
485 vidual has left the study area. However, this approach might produce ambiguous results in
486 cases where many individuals are released near map borders, especially because already a
487 single random step leaving the study area will break the simulation, thus resulting in biased
488 connectivity estimates along map borders. Rather than breaking the simulation, we created
489 a buffer zone (Koen et al., 2010) and resampled random steps until they fully lied within
490 the study area. This proved to be an effective solution to overcome problems with boundary

491 effects.

492 In summary, we proposed and applied a simple three-step approach that relies on ISSF-
493 analysis and enables the simulation of dispersal trajectories and the assessment of landscape
494 connectivity. The proposed approach overcomes several of the conceptual shortcomings
495 inherent to LCPA and CT, such as the assumption of known endpoints, and provides a highly
496 flexible tool for investigating connectivity. Moreover, the simulation of dispersal opens up
497 new avenues for incorporating interactions between habitat and movement covariates and
498 provides the foundation for a rich suite of complementary connectivity measures. With
499 this work, we hope to have sparked interest in the application, optimization, or creation
500 of methods to investigate dispersal and connectivity via individual-based simulations, while
501 at the same time stressing some of the non-trivial modeling decisions involved. We also
502 hope to provide a useful framework that helps unifying and streamlining the application of
503 individual-based simulations for assessing landscape connectivity.

504 **5 Authors' Contributions**

505 D.D.H., D.M.B., A.O. and G.C. conceived the study and designed methodology; D.M.B.,
506 G.C., and J.W.M. collected the data; D.D.H. and D.M.B. analysed the data; G.C. and A.O.
507 assisted with modeling; D.D.H., D.M.B., and G.C. wrote the first draft of the manuscript and
508 all authors contributed to the drafts at several stages and gave final approval for publication.

509 **6 Data Availability**

510 GPS movement data of dispersing wild dogs is available on dryad (Hofmann et al., 2021b).
511 Access to R-scripts that exemplify the application of the proposed approach using simulated
512 data are provided through Github (<https://github.com/DavidDHofmann/DispersalSimulation>).
513 In addition, all codes required to reproduce the African wild dog case study will be made
514 available through an online repository at the time of publication.

515 **7 Acknowledgements**

516 We thank the Ministry of Environment and Tourism of Botswana for granting permission
517 to conduct this research. We thank C. Botes, I. Clavadetscher, and G. Camenisch for
518 assisting with wild dog immobilizations. We also thank B. Abrahms for sharing her data
519 of three dispersing wild dogs. Furthermore, we would like to thank Johannes Signer for

520 assisting with the simulation algorithm. This study was funded by Albert-Heim Foundation,
521 Basler Stiftung für Biologische Forschung, Claraz Foundation, Idea Wild, Jacot Foundation,
522 National Geographic Society, Parrotia Stiftung, Stiftung Temperatio, Wilderness Wildlife
523 Trust, Forschungskredit of the University of Zürich (grant no. FK-21-091), and a Swiss
524 National Science Foundation grant (no. 31003A_182286) to A. Ozgul.

525 **8 Conflict of Interest**

526 All authors declare that they have no conflicts of interest.

527 References

- 528 Abrahms, B., Sawyer, S. C., Jordan, N. R., McNutt, J. W., Wilson, A. M., and Brashares,
529 J. S. (2017). Does Wildlife Resource Selection Accurately Inform Corridor Conservation?
530 *Journal of Applied Ecology*, 54(2):412–422.
- 531 Adriaensen, F., Chardon, J., De Blust, G., Swinnen, E., Villalba, S., Gulinck, H., and
532 Matthysen, E. (2003). The Application of Least-Cost Modelling as a Functional Landscape
533 Model. *Landscape and Urban Planning*, 64(4):233–247.
- 534 Allen, C. H., Parrott, L., and Kyle, C. (2016). An Individual-Based Modelling Approach to
535 Estimate Landscape Connectivity for Bighorn Sheep (*Ovis canadensis*). *PeerJ*, 4:e2001.
- 536 Avgar, T., Lele, S. R., Keim, J. L., and Boyce, M. S. (2017). Relative Selection Strength:
537 Quantifying Effect Size in Habitat- and Step-Selection Inference. *Ecology and Evolution*,
538 7(14):5322–5330.
- 539 Avgar, T., Potts, J. R., Lewis, M. A., and Boyce, M. S. (2016). Integrated Step Selection
540 Analysis: Bridging the Gap Between Resource Selection and Animal Movement. *Methods
541 in Ecology and Evolution*, 7(5):619–630.
- 542 Baguette, M., Blanchet, S., Legrand, D., Stevens, V. M., and Turlure, C. (2013). Individual
543 Dispersal, Landscape Connectivity and Ecological Networks. *Biological Reviews*,
544 88(2):310–326.
- 545 Bastille-Rousseau, G., Douglas-Hamilton, I., Blake, S., Northrup, J. M., and Wittemyer,
546 G. (2018). Applying Network Theory to Animal Movements to Identify Properties of
547 Landscape Space Use. *Ecological Applications*, 28(3):854–864.
- 548 Behr, D. M., McNutt, J. W., Ozgul, A., and Cozzi, G. (2020). When to Stay and When
549 to Leave? Proximate Causes of Dispersal in an Endangered Social Carnivore. *Journal of
550 Animal Ecology*, 89(10):2356–2366.
- 551 Brennan, A., Beytell, P., Aschenborn, O., Du Preez, P., Funston, P., Hanssen, L., Kilian,
552 J., Stuart-Hill, G., Taylor, R., and Naidoo, R. (2020). Characterizing Multispecies
553 Connectivity Across a Transfrontier Conservation Landscape. *Journal of Applied Ecology*,
554 57:1700–1710.
- 555 Brooks, M. E., Kristensen, K., van Benthem, K. J., Magnusson, A., Berg, C. W., Nielsen,
556 A., Skaug, H. J., Maechler, M., and Bolker, B. M. (2017). glmmTMB Balances Speed and
557 Flexibility among Packages for Zero-Inflated Generalized Linear Mixed Modeling. *The R
558 Journal*, 9(2):378–400.
- 559 Brown, J. H. and Kodric-Brown, A. (1977). Turnover Rates in Insular Biogeography: Effect
560 of Immigration on Extinction. *Ecology*, 58(2):445–449.
- 561 Burnham, K. P. and Anderson, D. R. (2002). *Model Selection and Multimodel Inference: A
562 Practical Information-Theoretic Approach*. Springer Science & Business Media, Ney York,
563 NY, USA.
- 564 Clark, J. D., Laufenberg, J. S., Davidson, M., and Murrow, J. L. (2015). Connectivity among
565 Subpopulations of Louisiana Black Bears as Estimated by a Step Selection Function. *The
566 Journal of Wildlife Management*, 79(8):1347–1360.
- 567 Clobert, J., Baguette, M., Benton, T. G., and Bullock, J. M. (2012). *Dispersal Ecology and
568 Evolution*. Oxford University Press, Oxford, UK.
- 569 Cozzi, G., Behr, D., Webster, H., Claase, M., Bryce, C., Modise, B., McNutt, J., and
570 Ozgul, A. (2020). The Walk of Life: African Wild Dog Dispersal and its Implications for
571 Management and Conservation across Transfrontier Landscapes. In press.
- 572 Cozzi, G., Broekhuis, F., McNutt, J. W., Turnbull, L. A., Macdonald, D. W., and Schmid,
573 B. (2012). Fear of the Dark or Dinner by Moonlight? Reduced Temporal Partitioning
574 among Africa's Large Carnivores. *Ecology*, 93(12):2590–2599.

- 575 Creel, S., Merkle, J., Mweetwa, T., Becker, M. S., Mwape, H., Simpamba, T., and
576 Simukonda, C. (2020). Hidden Markov Models Reveal a clear Human Footprint on the
577 Movements of Highly Mobile African Wild Dogs. *Scientific reports*, 10(1):1–11.
- 578 Csardi, G. and Nepusz, T. (2006). The igraph Software Package for Complex Network
579 Research. *InterJournal, Complex Systems*:1695.
- 580 Cushman, S. A., Elliot, N. B., Bauer, D., Kesch, K., Bahaa-el din, L., Bothwell, H., Flyman,
581 M., Mtare, G., Macdonald, D. W., and Loveridge, A. J. (2018). Prioritizing Core Areas,
582 Corridors and Conflict Hotspots for Lion Conservation in Southern Africa. *PLOS ONE*,
583 13(7):e0196213.
- 584 Davies-Mostert, H. T., Kamler, J. F., Mills, M. G. L., Jackson, C. R., Rasmussen, G. S. A.,
585 Groom, R. J., and Macdonald, D. W. (2012). Long-Distance Transboundary Dispersal
586 of African Wild Dogs among Protected Areas in Southern Africa. *African Journal of
587 Ecology*, 50(4):500–506.
- 588 Diniz, M. F., Cushman, S. A., Machado, R. B., and De Marco Júnior, P. (2019). Landscape
589 Connectivity Modeling from the Perspective of Animal Dispersal. *Landscape Ecology*,
590 35:41–58.
- 591 Doerr, V. A. J., Barrett, T., and Doerr, E. D. (2011). Connectivity, Dispersal Behaviour
592 and Conservation under Climate Change: A Response to Hodgson et al.: Connectivity
593 and Dispersal Behaviour. *Journal of Applied Ecology*, 48(1):143–147.
- 594 Dray, S., Royer-Carenzi, M., and Calenge, C. (2010). The Exploratory Analysis of Autocor-
595 relation in Animal-Movement Studies. *Ecological Research*, 25(3):673–681.
- 596 Eddelbuettel, D. (2013). *Seamless R and C++ Integration with Rcpp*. Springer, New York.
597 ISBN 978-1-4614-6867-7.
- 598 Eddelbuettel, D. and Balamuta, J. J. (2018). Extending extitR with extitC++: A Brief
599 Introduction to extitRcpp. *The American Statistician*, 72(1):28–36.
- 600 Eddelbuettel, D. and François, R. (2011). Rcpp: Seamless R and C++ Integration. *Journal
601 of Statistical Software*, 40(8):1–18.
- 602 Elliot, N. B., Cushman, S. A., Macdonald, D. W., and Loveridge, A. J. (2014). The Devil
603 is in the Dispersers: Predictions of Landscape Connectivity Change with Demography.
604 *Journal of Applied Ecology*, 51(5):1169–1178.
- 605 Fahrig, L. (2003). Effects of Habitat Fragmentation on Biodiversity. *Annual Review of
606 Ecology, Evolution, and Systematics*, 34(1):487–515.
- 607 Fieberg, J., Signer, J., Smith, B., and Avgar, T. (2021). A ‘How to’ Guide for Interpreting
608 Parameters in Habitat-Selection Analyses. *Journal of Animal Ecology*, 90(5):1027–1043.
- 609 Fortin, D., Beyer, H. L., Boyce, M. S., Smith, D. W., Duchesne, T., and Mao, J. S. (2005).
610 Wolves Influence Elk Movements: Behavior Shapes a Trophic Cascade in Yellowstone
611 National Park. *Ecology*, 86(5):1320–1330.
- 612 Fortin, D., Fortin, M.-E., Beyer, H. L., Duchesne, T., Courant, S., and Dancose, K. (2009).
613 Group-Size-Mediated Habitat Selection and Group Fusion–Fission Dynamics of Bison
614 under Predation Risk. *Ecology*, 90(9):2480–2490.
- 615 Frankham, R., Briscoe, D. A., and Ballou, J. D. (2002). *Introduction to Conservation
616 Genetics*. Cambridge University Press, Cambridge, UK.
- 617 Graves, T. A. and Waller, J. S. (2006). Understanding the Causes of Missed Global Posi-
618 tioning System Telemetry Fixes. *Journal of Wildlife Management*, 70(3):844–851.
- 619 Gustafson, E. J. and Gardner, R. H. (1996). The Effect of Landscape Heterogeneity on the
620 Probability of Patch Colonization. *Ecology*, 77(1):94–107.

- 621 Hanski, I. (1999). *Metapopulation Ecology*. Oxford University Press.
- 622 Hauenstein, S., Fattebert, J., Grüebler, M. U., Naef-Daenzer, B., Pe'er, G., and Hartig, F.
623 (2019). Calibrating an Individual-Based Movement Model to Predict Functional Connec-
624 tivity for Little Owls. *Ecological Applications*, 29(4):e01873.
- 625 Hijmans, R. J. (2021). *terra: Spatial Data Analysis*. R package version 1.2-10.
- 626 Hodel, F. H. and Fieberg, J. R. (2022). Circular-Linear Copulae for Animal Movement Data.
627 *Methods in Ecology and Evolution*, pages 2041–210X.13821.
- 628 Hofmann, D. D., Behr, D. M., McNutt, J. W., Ozgul, A., and Cozzi, G. (2021a). Bound
629 within boundaries: Do protected areas cover movement corridors of their most mobile,
630 protected species? *Journal of Applied Ecology*, 58(6):1133–1144. Publisher: Wiley Online
631 Library.
- 632 Hofmann, D. D., Behr, D. M., McNutt, J. W., Ozgul, A., and Cozzi, G. (2021b). Data from:
633 Bound within Boundaries: Do Protected Areas Cover Movement Corridors of their Most
634 Mobile, Protected Species? Dryad Digital Repository. [https://doi:10.5061/dryad.
635 dncjsxkzn](https://doi:10.5061/dryad.dncjsxkzn).
- 636 Kanagaraj, R., Wiegand, T., Kramer-Schadt, S., and Goyal, S. P. (2013). Using Individual-
637 Based Movement Models to Assess Inter-Patch Connectivity for Large Carnivores in Frag-
638 mented Landscapes. *Biological Conservation*, 167:298 – 309.
- 639 Koen, E. L., Bowman, J., Sadowski, C., and Walpole, A. A. (2014). Landscape Connectivity
640 for Wildlife: Development and Validation of Multispecies Linkage Maps. *Methods in
641 Ecology and Evolution*, 5(7):626–633.
- 642 Koen, E. L., Garroway, C. J., Wilson, P. J., and Bowman, J. (2010). The Effect of Map
643 Boundary on Estimates of Landscape Resistance to Animal Movement. *PLoS ONE*,
644 5(7):e11785.
- 645 Latham, A. D. M., Latham, M. C., Boyce, M. S., and Boutin, S. (2011). Movement Re-
646 sponses by Wolves to Industrial Linear Features and Their Effect on Woodland Caribou
647 in Northeastern Alberta. *Ecological Applications*, 21(8):2854–2865.
- 648 Leigh, K. A., Zenger, K. R., Tammen, I., and Raadsma, H. W. (2012). Loss of Genetic
649 Diversity in an Outbreeding Species: Small Population Effects in the African Wild Dog
650 (*Lycaon pictus*). *Conservation Genetics*, 13(3):767–777.
- 651 MacArthur, R. H. and Wilson, E. O. (2001). *The Theory of Island Biogeography*, volume 1.
652 Princeton University Press, Princeton, New Jersey, USA.
- 653 Martensen, A. C., Saura, S., and Fortin, M. (2017). Spatio-Temporal Connectivity: Assess-
654 ing the Amount of Reachable Habitat in Dynamic Landscapes. *Methods in Ecology and
655 Evolution*, 8(10):1253–1264.
- 656 Masenga, E. H., Jackson, C. R., Mjingo, E. E., Jacobson, A., Riggio, J., Lyamuya, R. D.,
657 Fyumagwa, R. D., Borner, M., and Røskraft, E. (2016). Insights into Long-Distance
658 Dispersal by African Wild Dogs in East Africa. *African Journal of Ecology*, 54(1):95–98.
- 659 McClintock, B. T., King, R., Thomas, L., Matthiopoulos, J., McConnell, B. J., and Morales,
660 J. M. (2012). A General Discrete-Time Modeling Framework for Animal Movement Using
661 Multistate Random Walks. *Ecological Monographs*, 82(3):335–349.
- 662 McClure, M. L., Hansen, A. J., and Inman, R. M. (2016). Connecting Models to Movements:
663 Testing Connectivity Model Predictions against Empirical Migration and Dispersal Data.
664 *Landscape Ecology*, 31(7):1419–1432.
- 665 McNutt, J. (1996). Sex-Biased Dispersal in African Wild Dogs (*Lycaon pictus*). *Animal
666 Behaviour*, 52(6):1067–1077.

- 667 McRae, B. H. (2006). Isolation by Resistance. *Evolution*, 60(8):1551–1561.
- 668 McRae, B. H., Dickson, B. G., Keitt, T. H., and Shah, V. B. (2008). Using Circuit Theory to
669 Model Connectivity in Ecology, Evolution, and Conservation. *Ecology*, 89(10):2712–2724.
- 670 Muff, S., Signer, J., and Fieberg, J. (2020). Accounting for Individual-Specific Variation in
671 Habitat-Selection Studies: Efficient Estimation of Mixed-Effects Models Using Bayesian
672 or Frequentist Computation. *Journal of Animal Ecology*, 89(1):80–92.
- 673 Osipova, L., Okello, M. M., Njumbi, S. J., Ngene, S., Western, D., Hayward, M. W., and
674 Balkenhol, N. (2019). Using Step-Selection Functions to Model landscape Connectivity
675 for African Elephants: Accounting for Variability across Individuals and Seasons. *Animal
676 Conservation*, 22(1):35–48.
- 677 O'Neill, H. M. K., Durant, S. M., and Woodroffe, R. (2020). What Wild Dogs Want: Habitat
678 Selection Differs across Life Stages and Orders of Selection in a Wide-Ranging Carnivore.
679 *BMC Zoology*, 5(1).
- 680 Perrin, N. and Mazalov, V. (2000). Local Competition, Inbreeding, and the Evolution of
681 Sex-Biased Dispersal. *The American Naturalist*, 155(1):116–127.
- 682 Pomilia, M. A., McNutt, J. W., and Jordan, N. R. (2015). Ecological Predictors of African
683 Wild Dog Ranging Patterns in Northern Botswana. *Journal of Mammalogy*, 96(6):1214–
684 1223.
- 685 Potts, J. R., Bastille-Rousseau, G., Murray, D. L., Schaefer, J. A., and Lewis, M. A. (2013).
686 Predicting local and non-local effects of resources on animal space use using a mechanistic
687 step selection model. *Methods in Ecology and Evolution*, 5(3):253–262.
- 688 R Core Team (2020). *R: A Language and Environment for Statistical Computing*. R Foun-
689 dation for Statistical Computing, Vienna, Austria.
- 690 Rudnick, D., Ryan, S., Beier, P., Cushman, S., Dieffenbach, F., Epps, C., Gerber, L., Hart-
691 ter, J., Jenness, J., Kintsch, J., Merenlender, A., Perkl, R., Perziosi, D., and Trombulack,
692 S. (2012). The Role of Landscape Connectivity in Planning and Implementing Conserva-
693 tion and Restoration Priorities. *Issues in Ecology*.
- 694 Sawyer, S. C., Epps, C. W., and Brashares, J. S. (2011). Placing Linkages among Fragmented
695 Habitats: Do Least-Cost Models Reflect How Animals Use Landscapes? *Journal of
696 Applied Ecology*, 48(3):668–678.
- 697 Signer, J., Fieberg, J., and Avgar, T. (2017). Estimating Utilization Distributions from
698 Fitted Step-Selection Functions. *Ecosphere*, 8(4):e01771.
- 699 Tischendorf, L. and Fahrig, L. (2000). On the Usage and Measurement of Landscape Con-
700 nectivity. *Oikos*, 90(1):7–19.
- 701 Turchin, P. (1998). *Quantitative Analysis of Movement: Measuring and Modeling Population
702 Redistribution in Plants and Animals*. Sinauer Associates, Sunderland, MA, USA.
- 703 Van der Meer, E., Fritz, H., Blinston, P., and Rasmussen, G. S. (2014). Ecological Trap in
704 the Buffer Zone of a Protected Area: Effects of Indirect Anthropogenic Mortality on the
705 African Wild Dog (*Lycaon pictus*). *Oryx*, 48(2):285–293.
- 706 Vasudev, D., Fletcher, R. J., Goswami, V. R., and Krishnadas, M. (2015). From Disper-
707 sal Constraints to Landscape Connectivity: Lessons from Species Distribution Modeling.
708 *Ecography*, 38(10):967–978.
- 709 Wolski, P., Murray-Hudson, M., Thito, K., and Cassidy, L. (2017). Keeping it Simple:
710 Monitoring Flood Extent in Large Data-Poor Wetlands Using MODIS SWIR Data. *In-
711 ternational Journal of Applied Earth Observation and Geoinformation*, 57:224–234.

- ⁷¹² Woodroffe, R., Rabaiotti, D., Ngatia, D. K., Smallwood, T. R. C., Strelbel, S., and O'Neill,
⁷¹³ H. M. K. (2019). Dispersal Behaviour of African Wild Dogs in Kenya. *African Journal
of Ecology*.
- ⁷¹⁵ Woodroffe, R. and Sillero-Zubiri, C. (2012). *Lycaon pictus*. *The IUCN Red List of Threatened
716 Species*, 2012:e. T12436A16711116.
- ⁷¹⁷ Zeller, K. A., Wattles, D. W., Bauder, J. M., and DeStefano, S. (2020). Forecasting Seasonal
718 Habitat Connectivity in a Developing Landscape. *Land*, 9(7):233.

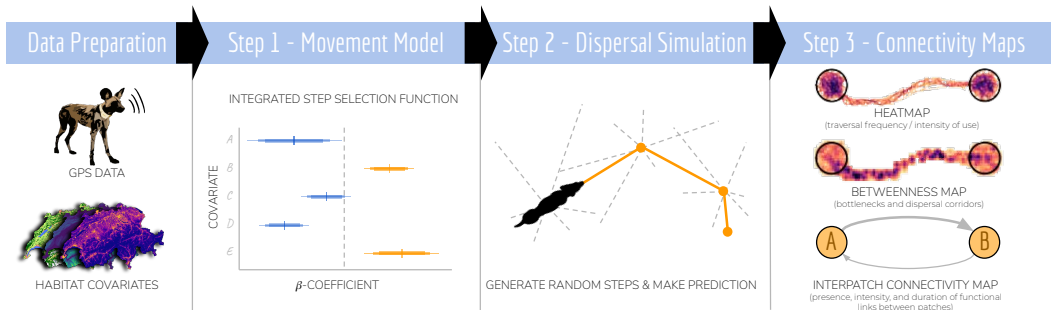


Figure 1: Flowchart of the simulation-based connectivity analysis. First, GPS data and habitat covariates must be collected. The combined data is then analyzed using an integrated step selection model. The parametrized model is then treated as an individual-based movement model and used to simulate dispersal trajectories. Ultimately, simulated trajectories are translated into a set of maps that are pertinent to landscape connectivity. This includes a heatmap, indicating the traversal frequency across each spatial unit of the study area, a betweenness map, highlighting movement corridors and bottlenecks, and, finally, an inter-patch connectivity map, where the frequency of connections and their average duration can be depicted.

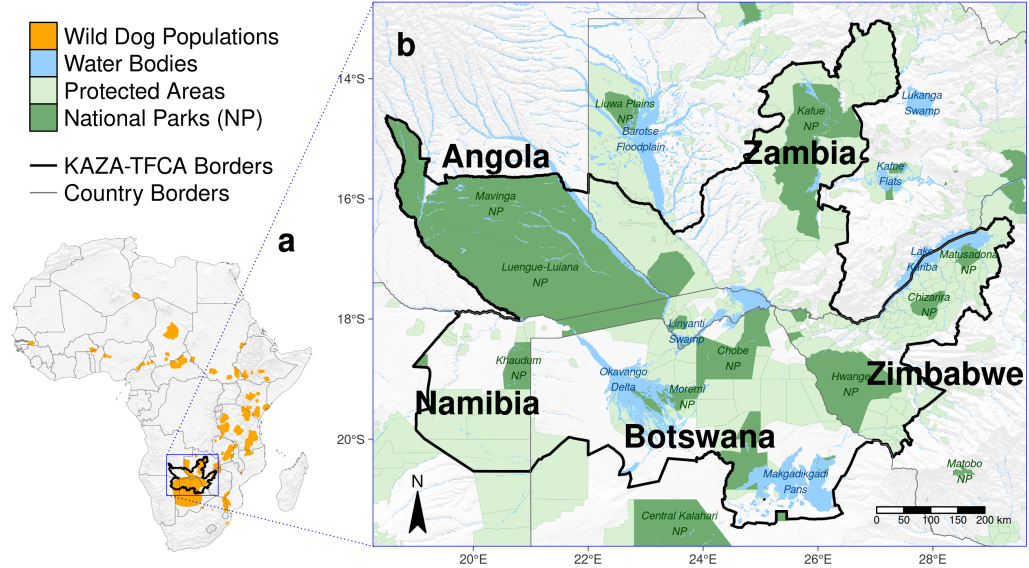


Figure 2: Illustration of the study area in southern Africa. (a) The study area was confined by a bounding box spanning the entire KAZA-TFCA which comprises parts of Angola, Namibia, Botswana, Zimbabwe, and Zambia. Data on remaining wild dog populations (orange) has been sourced from Woodroffe and Sillero-Zubiri (2012). (b) The KAZA-TFCA represents the world's largest terrestrial transfrontier conservation area and covers a total area of 520'000 km². Its main purpose is to re-establish connectivity between already-existing NPs (dark green) and other protected areas (light green).

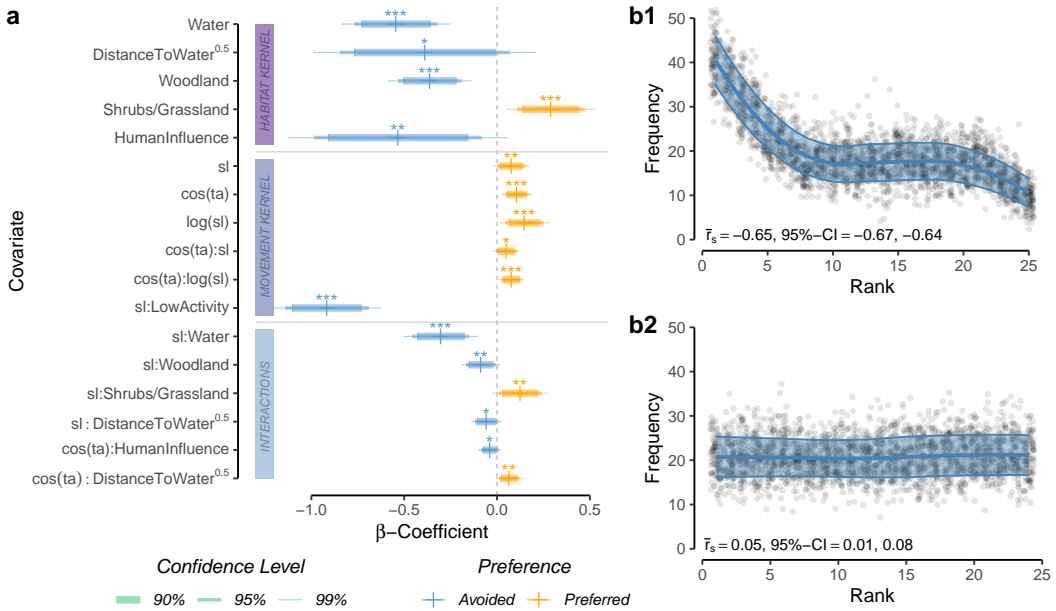


Figure 3: (a) Most parsimonious movement model for dispersing wild dogs. The model comprises a habitat kernel, a movement kernel, as well as their interactions. The horizontal line segments delineate the 90%, 95%, and 99% confidence-intervals for the respective β -coefficients. Significance codes: * $p < 0.10$, ** $p < 0.05$, *** $p < 0.01$. (b) Results from the k-fold cross validation procedure. The upper plot shows rank frequencies of realized steps according to model predictions with known preferences, whereas the lower plot shows rank frequencies of realized steps when assuming random preferences. The blue ribbon shows the prediction interval around a loess smoothing regression that we fitted to ease the interpretation of the plots. The significant correlation between rank and associated frequency in (b1) highlights that the most parsimonious model successfully outperformed a random guess (b2) and assigned high selection scores to realized steps.

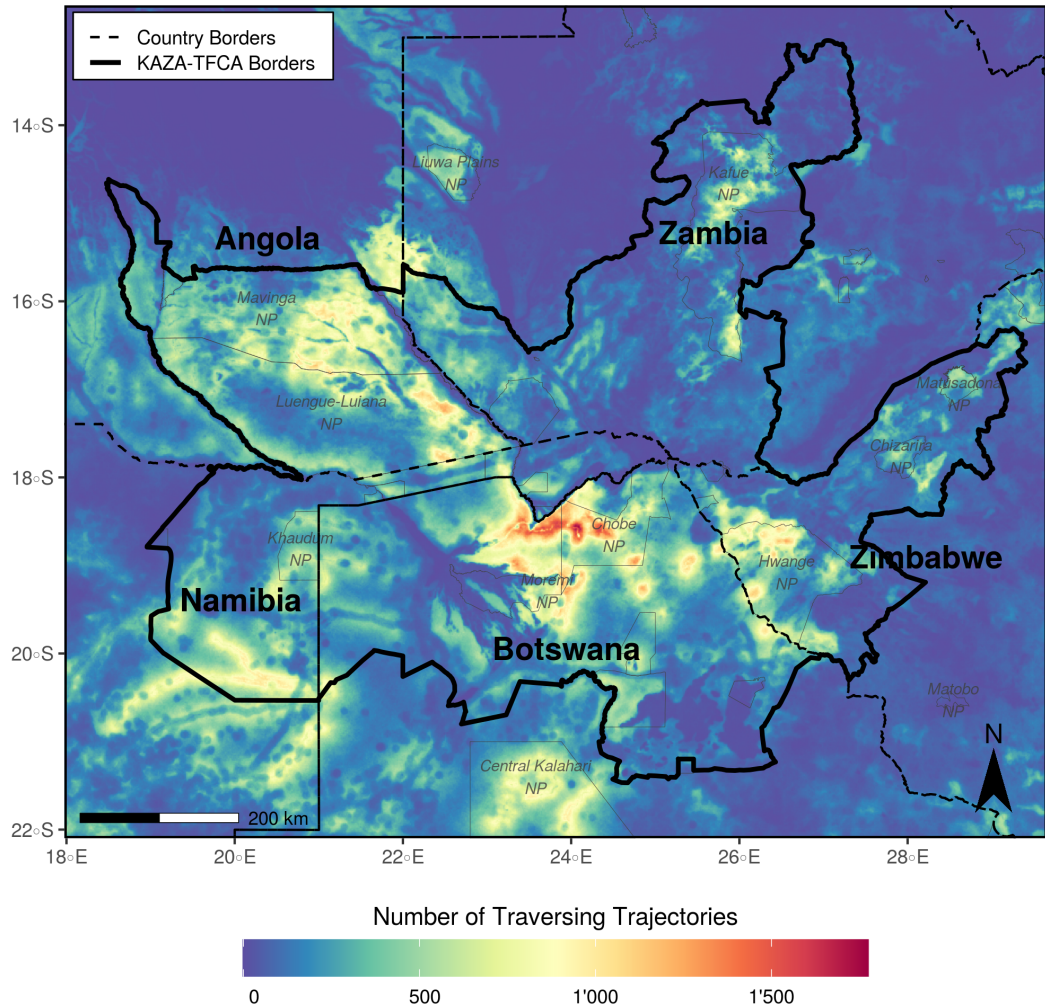


Figure 4: Heatmap showing traversal frequencies of 80'000 simulated dispersers moving 2'000 steps across the KAZA-TFCA. Simulations were based on an integrated step-selection model that we fitted to the movement data of dispersing African wild dogs. To generate the heatmap, we rasterized and tallied all simulated trajectories. Consequently, the map highlights areas that are frequently traversed. For spatial reference we plotted a few selected NPs (dark gray). Additional heatmaps showing the traversal frequency when individuals move fewer than 2'000 steps are provided in Figure S4.

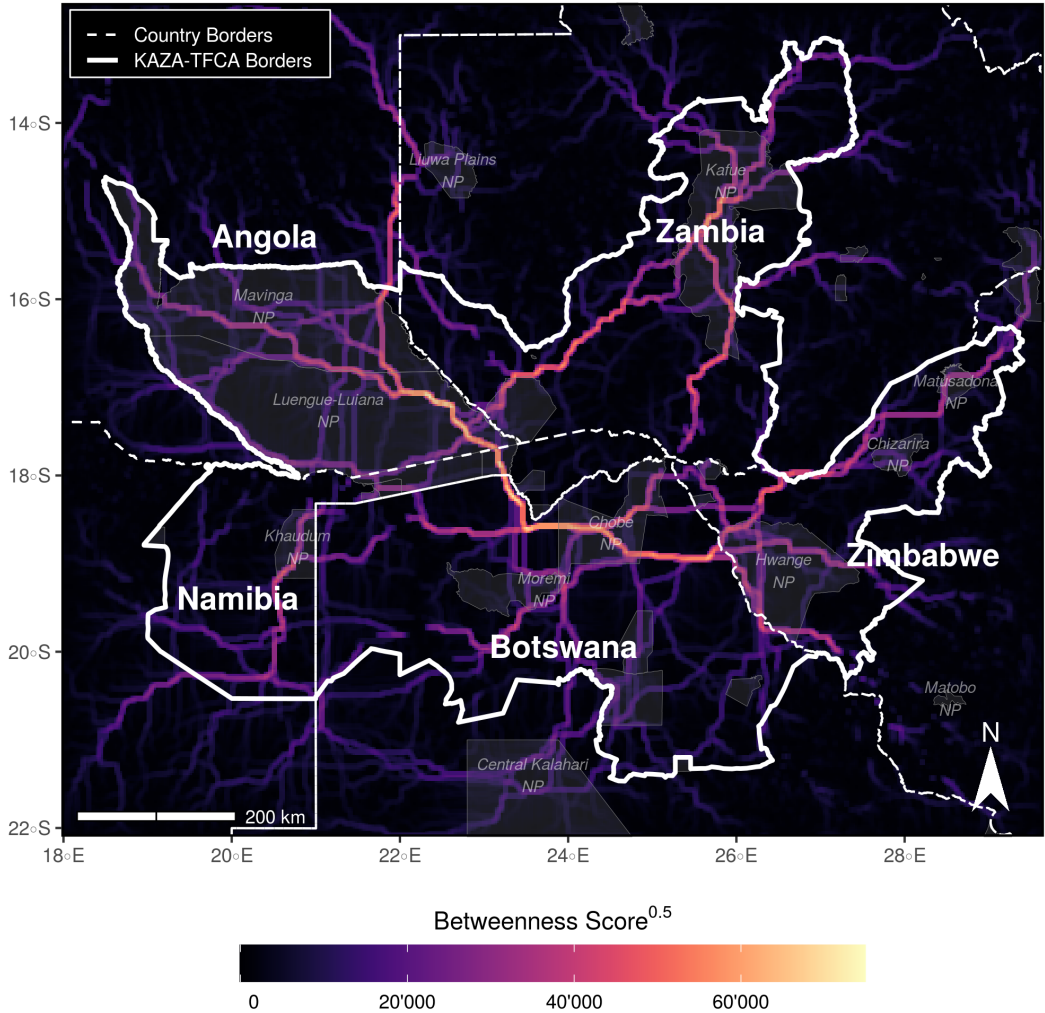


Figure 5: Map of betweenness scores, highlighting distinct dispersal corridors and potential bottlenecks across the extent of the KAZA-TFCA. Betweenness measures the number of shortest paths traversing through each node (raster-cell). Hence, a high betweenness score indicates that the respective area is exceptionally important for connecting different regions in the study area. The metric is therefore useful to pinpoint discrete movement corridors (Bastille-Rousseau et al., 2018). Note that we square-rooted betweenness scores to improve visibility of corridors with comparably low scores. Additional betweenness maps showing betweenness scores when individuals move fewer than 2'000 steps are provided in Figure S4.

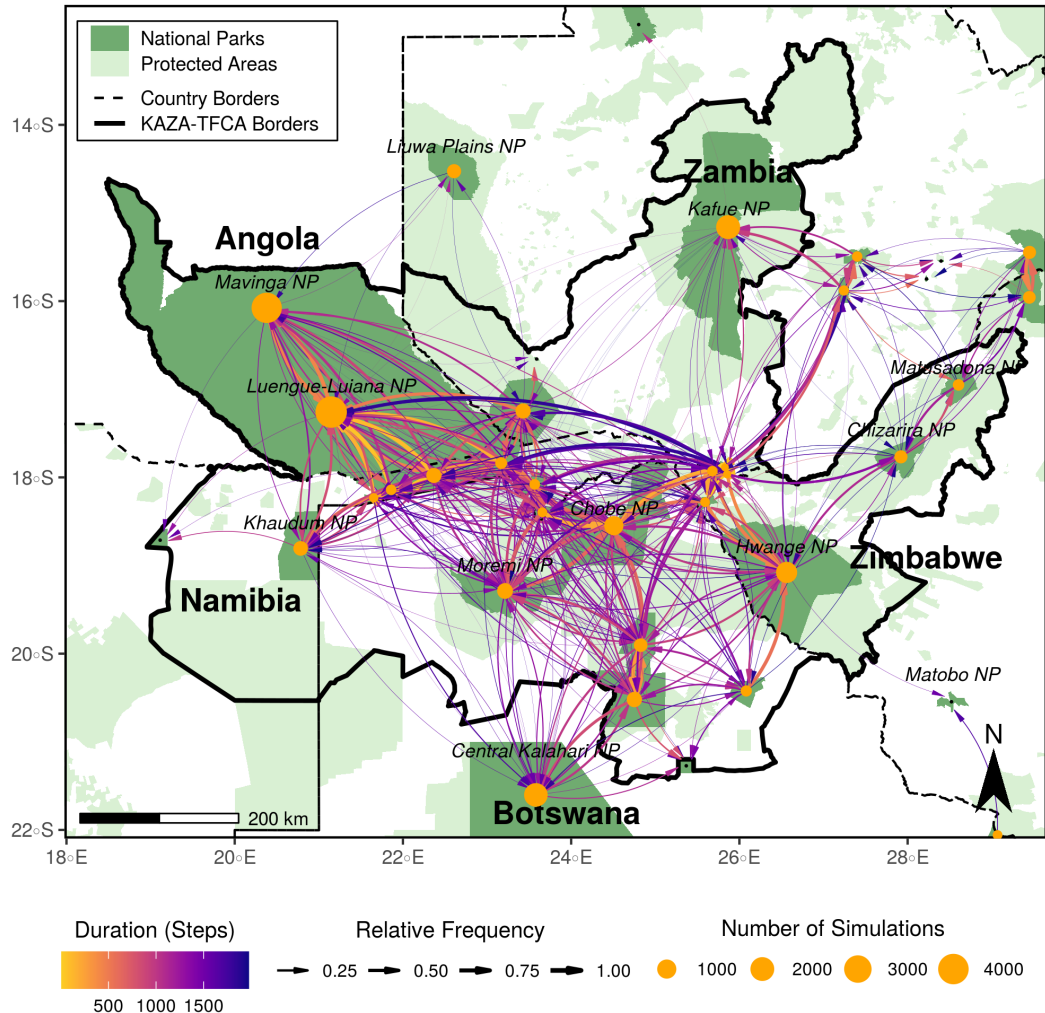


Figure 6: Map of inter-patch connectivity in relation to dispersal duration, highlighting connections between NPs (dark green). Yellow bubbles represent the center of the different NPs and are sized in relation to the number of simulated dispersers originating from each park. Black dots represent NPs that were smaller than 700 km^2 and therefore were not used as source areas. Arrows between NPs illustrate between which NPs the simulated dispersers successfully moved and the color of each arrow shows the average number of steps (i.e. 4-hourly movements) that were necessary to realize those connections. Additionally, the line thickness indicates the relative number of dispersers originating from a NP that realized those connections.